

# Palmitate-mediated disruption of the endoplasmic reticulum decreases intracellular vesicle motility

Nathan T. Rayens, 1 Keisha J. Cook, 2 Scott A. McKinley, 3 and Christine K. Payne 1,\*

<sup>1</sup>Thomas Lord Department of Mechanical Engineering and Materials Science, Duke University, Durham, North Carolina; <sup>2</sup>School of Mathematical and Statistical Sciences, Clemson University, Clemson, South Carolina; and <sup>3</sup>Department of Mathematics, Tulane University, New Orleans, Louisiana

ABSTRACT Essential cellular processes such as metabolism, protein synthesis, and autophagy require the intracellular transport of membrane-bound vesicles. The importance of the cytoskeleton and associated molecular motors for transport is well documented. Recent research has suggested that the endoplasmic reticulum (ER) may also play a role in vesicle transport through a tethering of vesicles to the ER. We use single-particle tracking fluorescence microscopy and a Bayesian change-point algorithm to characterize vesicle motility in response to the disruption of the ER, actin, and microtubules. This high-throughput change-point algorithm allows us to efficiently analyze thousands of trajectory segments. We find that palmitate-mediated disruption of the ER leads to a significant decrease in vesicle motility. A comparison with the disruption of actin and microtubules shows that disruption of the ER has a significant impact on vesicle motility, greater than the disruption of actin. Vesicle motility was dependent on cellular region, with greater motility in the cell periphery than the perinuclear region, possibly due to regional differences in actin and the ER. Overall, these results suggest that the ER is an important factor in vesicle transport.

SIGNIFICANCE Cells require intracellular transport of vesicles to function. We have used fluorescence microscopy to track the motion of vesicles and a new Bayesian change-point algorithm to analyze the motion. While much previous research has investigated the actin and microtubule cytoskeleton, this work provides the first experiments measuring the motility of vesicles as a function of palmitate-mediated ER disruption. Surprisingly, we find that structural changes to the ER significantly decrease vesicle motility. This indicates that the ER is an important organelle to consider in our understanding of intracellular transport.

# INTRODUCTION

Cells require vesicle-mediated intracellular transport for a wide range of functions (1–4). These functions include metabolism (5–7), protein synthesis (8–10), cell division (11–13), neuron activity (14–17), autophagy (18–20), and wound healing (21–23). Diseases such as Alzheimer's, Huntington's, and cystinosis are associated with disrupted intracellular transport (24–32). Vesicle transport includes microtubule-dependent motion with kinesin and dynein motor proteins moving vesicles along microtubules and myosin motors moving cargo along actin filaments (33–42). Beyond the well-studied role of molecular motors and cytoskeletal transport, vesicle size (43–45), macromo-

Submitted September 23, 2022, and accepted for publication February 28, 2023.

\*Correspondence: christine.payne@duke.edu

Editor: Jeanne Stachowiak.

https://doi.org/10.1016/j.bpj.2023.03.001

© 2023 Biophysical Society.

lecular crowding (46–49), and endoplasmic reticulum (ER)-vesicle interactions (50–55) have been investigated as factors in intracellular transport.

Intracellular transport in live cells is measured using fluorescence microscopy and single-particle tracking. Single-particle tracking analysis, including our own (44), has relied on fitting of mean-square displacement (MSD) curves to classify vesicle motion as subdiffusive, diffusive, or active (56-61). Recent work has demonstrated that MSDs are limited both by measurement error and appropriate maximum lag (62-64). To address these concerns, numerous inferential particle tracking analysis approaches have been implemented (65-72). Among these, we recently described a Bayesian change-point analysis for single-particle tracking in live cells (45). The advantage of this method is the segmentation of trajectories into individual states defined by their speed. For vesicle trafficking, we can directly export data from TrackMate (73), use change-point analysis to segment trajectories, and perform rigorous



statistical inference of motion states across experiments for high-throughput characterization of thousands of trajectories.

We now use this high-throughput change-point analysis method to address the underlying biophysics of vesicle-mediated transport using ~7000–30,000 trajectory segments for each experimental condition. We use fluorescently labeled dextran, a polysaccharide internalized into vesicles by pinocytosis, to label vesicles (74–76). We first demonstrate the use of our method by measuring transport following disruption of actin filaments and microtubules. As expected, intracellular transport is decreased. We then measure the effect of two cellular structures that have recently been proposed to affect intracellular transport: the ER and ribosomes (50–55,77).

The ER has been shown to be important for the positioning of endolysosomal vesicles (50,51). ER structure can be disrupted through cisternal expansion induced by high concentrations of palmitate, a fatty acid (78–82). We use palmitate to disrupt the ER and investigate how this structural change influences vesicle transport. Recent work from Delarue et al. has shown that ribosomes serve as cytosolic crowding agents by contributing  $\sim$ 20% of the cytosolic volume (77). We use a similar approach, decreasing ribosomal concentration with rapamycin, and then measure vesicle motility.

These experiments led to an interesting new result. Vesicle motility is significantly reduced in response to palmitate-mediated ER disruption. The ER was found to be significantly more important than actin filaments in maintaining vesicle motility. Microtubules, as expected, were found to be the most important component for vesicle motility. We saw no effect of decreased ribosomal concentration on vesicle transport. The increased lysosomal motility in the cell periphery, observed in our previous work (45), is also observed with these dextran-labeled vesicles and discussed in terms of actin and ER localization. Overall, this work, enabled by a high-throughput Bayesian change-point analysis, shows that the structure of the ER is a key factor in vesicle motility.

#### MATERIALS AND METHODS

### Cell culture and fluorescent labeling of vesicles

Monkey kidney epithelial cells (BS-C-1, obtained from the Duke University Cell Culture Facility) were cultured in Dulbecco's modified Eagle medium (#12100046, Thermo Fisher Scientific, Waltham, MA, USA). Cell culture media were supplemented with 10% fetal bovine serum (#10437028, Thermo Fisher Scientific). Cells were incubated at 37°C with 5% carbon dioxide. Cells were passaged with trypsin (#25200072, Thermo Fisher Scientific) every 2–3 days. For imaging experiments, 35 mm optical dishes were used (#150682, Thermo Fisher Scientific).

Vesicles were labeled with tetramethylrhodamine-dextran, (10 kDa, 0.25 mg/mL, 18-24 h incubation, #D1817, Thermo Fisher Scientific). Dextran is internalized pinocytically, labeling vesicles nonspecifically (74-76). In comparison, our previous work was limited to lysosomes

(45). Colocalization measurements with emerald green fluorescent protein (GFP)-lysosome associated membrane protein 1 were carried out to characterize the dextran-containing vesicles (Fig. S1). Cells were transduced with CellLight Lysosomes-GFP (1:200, BacMam 2.0, #C10596; Thermo Fisher Scientific) according to the supplier's instructions. 3 h after the start of the BacMam incubation, dextran (0.25 mg/mL) was added to the cell culture media. 18 h later, the cells were washed with phosphate-buffered saline (PBS; #21300-025, Thermo Fisher Scientific) and imaged in PBS using the GFP and red fluorescent protein channels, as described below. For static images that included nuclear staining, 4',6-diamidino-2-phenylindole was used (50  $\mu$ M in PBS, room temperature [RT] for 30 min, #10236276001, Sigma-Aldrich).

# Drug treatments to disrupt actin, microtubules, ER, and ribosomes

Cytochalasin D (cytoD; 2 µM, 30 min, #C8273, Sigma-Aldrich) was used to inhibit actin filament polymerization (83,84). Disruption of actin filaments was confirmed using fluorescently labeled phalloidin (ActinRed rhodamine phalloidin, #R37112, Thermo Fisher Scientific). Cells were fixed with 4% paraformaldehyde (#15710, Electron Microscopy Services, Hatfield, PA, USA) in PBS for 10 min at RT. Cells were then washed with PBS and permeabilized (10% fetal bovine serum, 3% bovine serum albumin [BSA] (#A2153, Sigma-Aldrich), 0.00005% Triton-X 100 (#T8787, Sigma-Aldrich)) in PBS for 3–5 min at RT. Cells were then incubated with phalloidin (1:1500) at RT for 15 min before washing three times and imaging in PBS.

Nocodazole (2.2  $\mu$ M, 30 min, #M1404-10MG, Sigma-Aldrich) was used to inhibit microtubule polymerization (85–87). Disruption of microtubules was confirmed using immunofluorescence, as described below.

The ER was disrupted using palmitate (0.5 mM, 4 h) as shown in previous work (78–82). Palmitate (#P9767, Sigma-Aldrich) was solubilized through complexation with fatty acid-free BSA (#A6003, Sigma-Aldrich) in an NaCl (#S7653, Sigma-Aldrich) solution (88). The only modification to this protocol was an increased concentration of palmitate to make 5 mM palmitate-BSA aliquots, maintaining the ratio of palmitate: albumin. To visualize ER disruption, ER-Tracker Red (0.66  $\mu$ M, #E34250, Thermo Fisher Scientific) was applied to live cells following supplier's instructions.

Ribosomal concentration was decreased using rapamycin (1.5  $\mu$ M, 3 h, #R8781-200uL, Sigma-Aldrich) as shown previously (77). Rapamycin blocks mammalian target of rapamycin (89,90). Mammalian target of rapamycin signaling results in the phosphorylation of ribosomal protein S6 producing phospho-S6 (P-S6) (91,92). Immunofluorescence of P-S6 was used to confirm rapamycin activity, as described below.

Cell health following drug treatments was confirmed with the 3-(4,5-dimethylthiazol-2-yl)-2,5-diphenyltetrazolium bromide (MTT) assay (#V13154, Thermo Fisher Scientific) according to the supplier's instructions. Cytoskeleton- and ribosome-disrupting drugs caused no change in cell viability (Fig. S2 A). In addition, no decrease in viability was observed following palmitate treatment (Fig. S2 B). The intracellular distribution of vesicles was unchanged with drug treatments (Fig. S3).

Cellular ATP concentration was quantified using a firefly luciferase assay (#SCT149, Sigma-Aldrich) following the supplier's instructions. None of the treatments resulted in a significant decrease of ATP (Fig. S4).

#### Immunofluorescence of microtubules and P-S6

Immunofluorescence was used to image microtubules and the P-S6 ribosomal protein to confirm disruption by nocodazole and rapamycin, respectively. Fixation and permeabilization are described above for phalloidin staining. Following permeabilization, cells were washed with PBS and blocked (10% goat serum [#16210064, Thermo Fisher Scientific], 3% BSA in PBS) for 1 h at RT. The blocking buffer was then removed and replaced with fresh blocking buffer and the primary antibody (1:1000). The cells were stained for 3–18 h at RT and washed with PBS. The secondary antibody was added to fresh blocking buffer (3–18 h, RT).

For visualization of microtubules, mouse anti-α-tubulin (1:1000, #ab7291, Abcam, Cambridge, UK) was used as the primary antibody and goat anti-mouse (1:1000, Alexa Fluor 568, #ab175473, Abcam) as the secondary antibody. For P-S6, rabbit anti-P-S6 (1:1000, #MA5-15140, Thermo Fisher Scientific) was used as the primary antibody and goat anti-rabbit (1:1000, Alexa Fluor 488, #ab150077, Abcam) as the secondary antibody.

### Live-cell imaging and single-particle tracking

Live-cell imaging and single-particle tracking were used to observe and characterize lysosome motion. Live-cell imaging was carried out using a spinning disk confocal microscope (IX-81 [Olympus], CSU-X1 confocal scanning unit [Yokogawa, Tokyo, Japan], iXon X3 camera [Andor], and MetaMorph v.7.8.2.0 software [Molecular Devices, San Jose, CA, USA]). Images were collected using the red fluorescent protein excitation filter, with the stream function (MetaMorph) used to control exposure time, field-of-view area, and gain for the desired frame rate. Vesicle transport in these thin ( $\sim$ 5  $\mu$ m) epithelial cells is approximately two-dimensional (93). Motion in the z-dimension would cause vesicles to move in and out of the focal plane during tracking. This was not observed. Time-lapse images were exported to FIJI (v.2.0.0-rc-69./1.52p), noise was removed with the despeckling filter, and vesicles were tracked with the TrackMate plugin (73). To remove selection bias, a random number generator was used to select 100 trajectories from each cell. The perinuclear region was defined by identifying the nucleus in bright-field images and defining a border between the densely packed vesicles and the sparser population in the periphery.

### Analysis of motility

Using our previously developed Bayesian change-point segmentation model (45), vesicle trajectories were segmented into individual trajectory segments using the bcp package in R (94) to select the most common number of predicted change points estimated per trajectory, to connect those change points linearly, and then to minimize the variation between the reconstructed and original trajectories. If a segment contained more than five steps and had a speed >100 nm/s, that segment was characterized as motile. Slower segments were labeled stationary. Unlike with MSD curve fitting, motile is a descriptive label of inferred speed and not a specific

type of motion. As such, the term motile can encompass both directed transport and fast diffusion of vesicles. For comparison across drug treatments, average motility was normalized to control values from untreated cells. Average motility estimates of trajectory segments are presented along with unnormalized data from individual cells.

### RESULTS AND DISCUSSION

# Disruption of actin and microtubules decreases vesicle motility

The importance of actin and microtubules for intracellular transport is well understood (33–42). To provide a comparison to ER disruption, we used cytoD and nocodazole to inhibit actin and microtubule polymerization, respectively. For each condition, we report both averaged values for all trajectory segments ( $n \approx 20,000$ ) and results from individual cells ( $n \approx 70$ ), showing similar effects. Confidence intervals (CIs, 95%) for each estimate are included in square brackets. Comparisons are considered significant if CIs do not overlap.

CytoD (2  $\mu$ M, 30 min) prevents polymerization of actin subunits into filaments (Fig. 1, A and B) (83,84). Estimating from trajectory segments, we observed a small, significant reduction of vesicle motility compared with untreated control cells (Fig. 1 C; control = 100% [96.6 103.6], normalized; cytoD treated = 79.3% [76.2 82.3]; [95% CIs]). A similar reduction of motility (15.3%–12.3%, unnormalized) was also observed averaging over individual cells (Fig. 1 D).

Nocodazole (2.2  $\mu$ M, 30 min) prevents polymerization of tubulin subunits to form microtubules (Fig. 2, A and B) (85–87). Estimating from trajectory segments, we found a large reduction of vesicle motility compared with untreated control cells (Fig. 2 C; control = 100% [96.6103.6], nocodazole treated = 45.8% [43.6 48.1]; [95% CIs]). A similar reduction of motility (15.6%–7.2%, unnormalized) was also observed when averaging over individual cells (Fig. 2 D).

As expected, both cytoD and nocodazole significantly reduced motility through cytoskeletal disruptions.

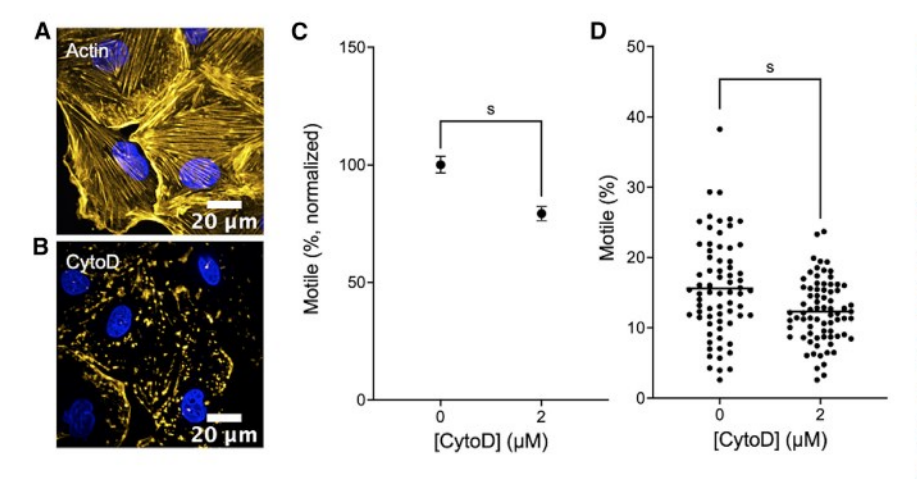


FIGURE 1 Inhibition of actin polymerization decreases vesicle motility. (A) Untreated control cells. Actin is labeled with phalloidin (yellow) and nuclei with 4',6-diamidino-2-phenylindole (DAPI; blue). (B) CytoD-treated cells (2 µM, 30 min). (C) Vesicle motility in control (n =26,038 segments from 7000 trajectories) and cytoD-treated (n = 23,776 segments from 7491 trajectories) cells. The average (normalized) estimated segment motility is shown. Error bars show 95% CIs. Significance is determined by CIs that do not overlap. (D) Vesicle motility for individual cells (n = 70 control cells and 75 cytoD-treated cells from 15 experiments). Horizontal lines show means. The significance comparison is taken directly from population-level 95% CIs in (C). To see this figure in color, go online.

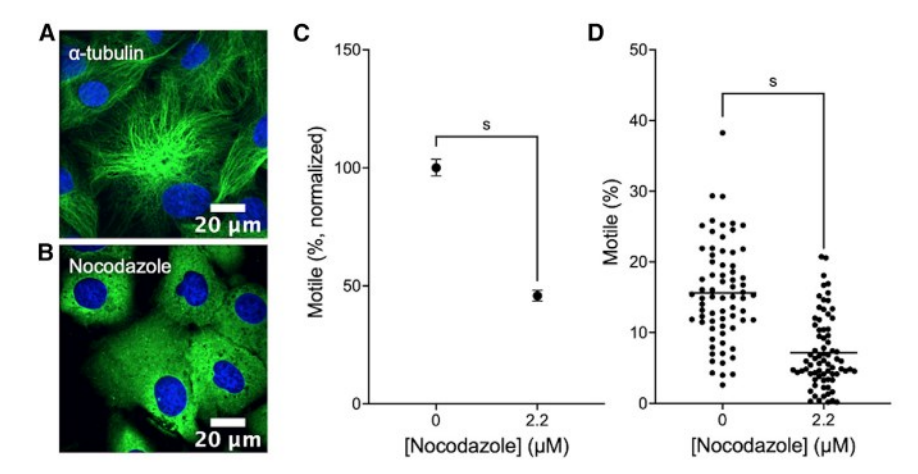


FIGURE 2 Disruption of microtubules decreases motility. (A) Untreated control cells. α-Tubulin (green) is labeled by immunofluorescence and nuclei with DAPI (blue) (B) Nocodazole-treated cells (2.2 µM, 30 min). (C) Vesicle motility in control (n = 26,038 segments from 7000 trajectories, control data are replotted from Fig. 1) and nocodazole-treated (n = 19,823 segments from 7390 trajectories) cells. The average (normalized) of estimated segment motility is shown. Error bars show 95% CIs. Significance is determined by CIs that do not overlap. (D) Vesicle motility for individual cells (n = 70 control and 74 nocodazoletreated cells from 15 experiments). Horizontal lines show means. The significance comparison is taken directly from population-level 95% CIs in (C). To see this figure in color, go online.

Following the inhibition of actin polymerization with cytoD, the remaining 79.3% motility is likely a combination of fast diffusion, remaining actin-based transport, and microtubule-based motion, which is not affected by cytoD. Similarly, when microtubules are disrupted, the remaining 45.8% motility could be attributed to fast diffusion, nocodazole-resistant microtubules (95), and unaltered actin-based transport. Although nocodazole can result in the fragmentation of the Golgi (95), the observed decrease in motility is in agreement with previous work showing that microtubule disruption leads to decreased vesicle transport (33,35,36,38).

# Disruption of ER decreases motility

The ER plays a key role in the positioning of vesicles (50-52). To determine the influence of ER-vesicle interactions on vesicle motility, we disrupted the ER using palmitate (78–82,88). Palmitate-induced lipid saturation causes cisternal ER expansion (81). The ER expansion is visible in fluorescently labeled cells (Fig. 3, A and B). We found that disruption of the ER with palmitate (0.5 mM) led to a reduction of motility (Fig. 3 C, control = 100% [96.7 103.3], palmitate treated = 69.3% [66.4 72.3]; [95% CIs]). This decrease in motility was also seen when averaging over individual cells (Fig. 3 D, 19.7% and 13.4%, unnormalized).

In addition to expansion of the ER, palmitate leads to ER stress associated with mitochondrial dysfunction (96-98), depletion (99-101), and increased apoptosis (78,97,102). We confirmed that there was no significant loss of cell viability with an MTT assay and no significant decrease in ATP using a luminescence assay (Figs. S2 and S4). This suggests that the decreased motility is due to the cisternal expansion of the ER.

# Reduced ribosomal concentration does not alter motility

Ribosomes are the macromolecular cellular structures responsible for protein synthesis (1,103). Recent work has demonstrated that ribosomes serve as crowding agents in the cytosol and that rapamycin decreases ribosomal concentration (77), in addition to a host of metabolic and catabolic effects (104,105). As macromolecular crowding can limit

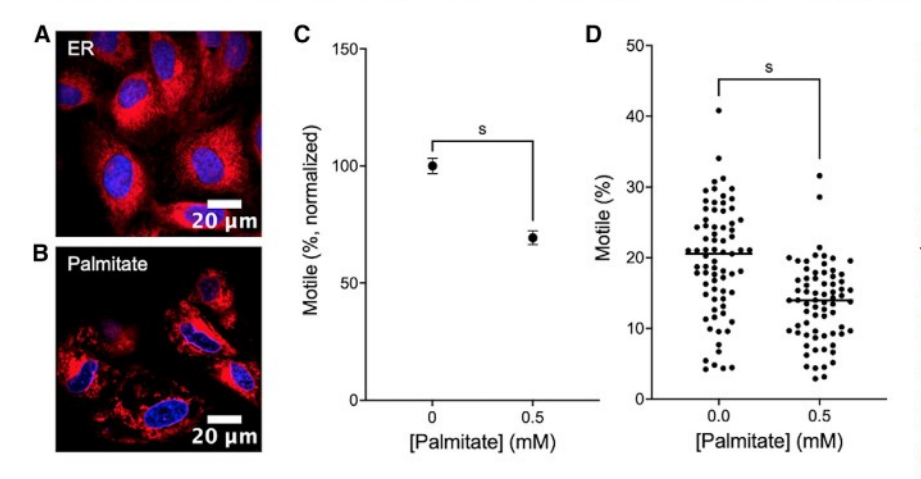


FIGURE 3 ER disruption decreases vesicle motility. (A) Untreated control cells. The ER is labeled with ER-Tracker dye (red) and nuclei with DAPI (blue). (B) Palmitate-treated cells (0.5 mM, 4 h). (C) Vesicle motility in control (n = 26,257 segments from 7300 trajectories)and 0.5 mM (n = 19,797 segments from 7000 trajectories) palmitate-treated cells. The average (normalized) of estimated segment motility is shown. Error bars show 95% CIs. Significance is determined by CIs that do not overlap. (D) Vesicle motility for individual cells (n = 73 control and 70 0.5 mM palmitate-treated cells from 15 experiments). Horizontal lines show means. The significance comparison is taken directly from population-level 95% CIs in (C). To see this figure in color, go online.

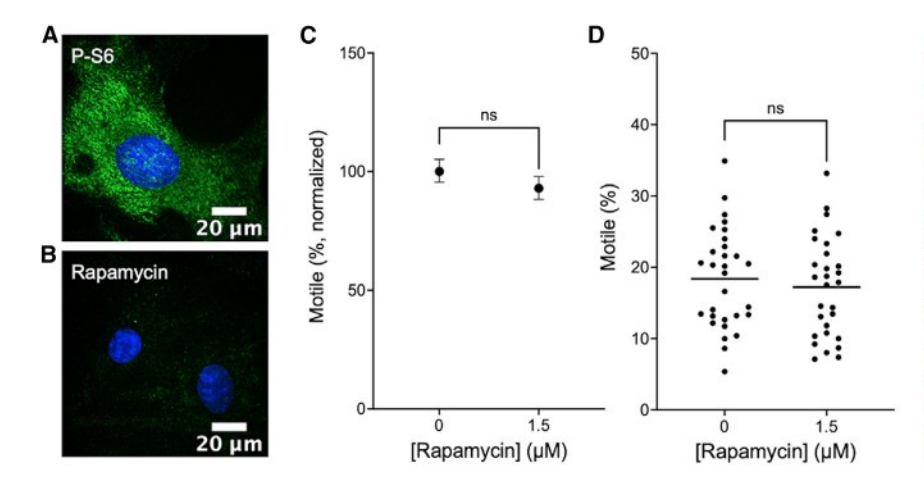


FIGURE 4 Decreased ribosomal concentration does not alter vesicle motility. (A) Untreated control cells with P-S6 (green) labeled by immunofluorescence and nuclei labeled with DAPI (blue). (B) Rapamycin-treated cells (1.5 µM, 3 h). (C) Vesicle motility in control (n = 12,591 segments from 3000 trajectories) and rapamycin-treated (n = 11,543 segments from 2900 trajectories) cells. The average (normalized) of estimated segment motility is shown. Error bars show 95% CIs. Significance is determined by CIs that do not overlap. (D) Vesicle motility for each imaging location (n = 30 control and 29 rapamycin-treated cells total from 6 experiments). Horizontal lines show means. The significance comparison is taken directly from population-level 95% CIs in (C). To see this figure in color, go online.

diffusion in the cytosol (46-49), we measured vesicle motility following treatment of cells with rapamycin to decrease the concentration of ribosomes. Using immunofluorescence, we confirmed that rapamycin decreases P-S6 (Fig. 4, A and B), a ribosomal protein that serves as a marker for rapamycin activity and decreased concentration of ribosomes (77). We found that there was no significant change to vesicle motility with reduced ribosomal concentration (Fig. 4 C). Similarly, no change was observed when averaging over multiple cells (Fig. 4 D). In comparison, Delarue et al. observed a significant increase to the effective diffusion coefficients of particles >20 nm in diameter. This difference may be due to differences in the specific type of particle tracked. Our experiments measure the intracellular transport of endogenous vesicles, mostly lysosomes (Fig. S1), rather than the diffusion of genetically introduced protein particles tracked by Delarue et al. The endogenous vesicles, compared with the protein particles, are transported by motor proteins along the cytoskeleton, while the protein particles are limited to passive diffusion within the cell.

It should be noted that in addition to regulating ribosome concentration, rapamycin has broad effects on cell metabolism and has been shown to significantly decrease cell viability (106,107). We used an MTT assay to confirm that rapamycin did not decrease cell viability (Fig. S2). Additionally, we confirmed that the rapamycin treatment did not deplete cellular ATP (Fig. S4).

# ER and microtubules have the greatest impact on vesicle motility

Using the normalized change in motility, we can examine the relative impact of the disruption of actin, microtubules, the ER, and ribosomal concentration on overall vesicle motility (Fig. 5). Loss of actin and microtubules reduces motility by 20.7% [17.7 23.8] and 54.2% [51.9 56.4], respectively (Figs. 1 and 2). Disruption of the ER reduces motility by 30.7% [27.7 33.6] (Fig. 3). Decreasing ribo-

somal concentration caused a 7% reduction [2.1 11.7] (Fig. 4), although this was not statistically significant. These contributions are not additive, as different types of motion contribute to motility. For example, fast diffusion and actin comet motion (108–110), independent of microtubules, would be classified as motile. Interestingly, these results show that palmitate-mediated disruption of the ER has the second most significant impact on vesicle motility.

# Comparison of perinuclear and peripheral vesicle motility

Our previous work identified a regional difference in lysosomal transport with greater motility of lysosomes in the periphery of the cell compared with the perinuclear region. The same trend is observed here with tracking of dextran-labeled vesicles rather than specifically tracking lysosomes (Fig. 6 A; periphery = 100% [97.3 102.7], perinuclear = 77.1% [74.6 79.7]; [95% CI]). This regional dependence was also observed for individual cells (20.6%–14.9%, unnormalized). Although not probed directly, the regional differences in motility may

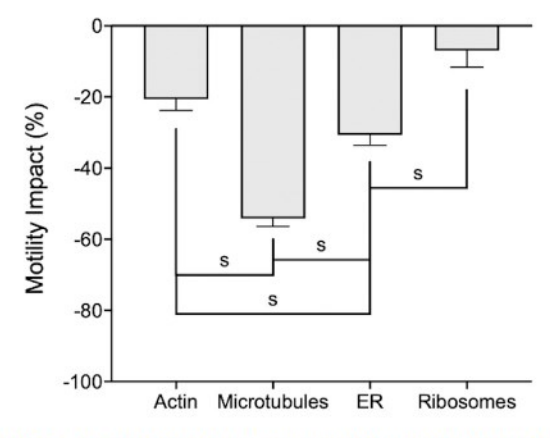


FIGURE 5 Comparison of decrease in vesicle motility due to disruption of the cytoskeleton, ER, and ribosomes. Error bars show normalized 95% CIs. Significance is determined by CIs that do not overlap. Disruption of microtubules and ER have the greatest impact on vesicle motility.

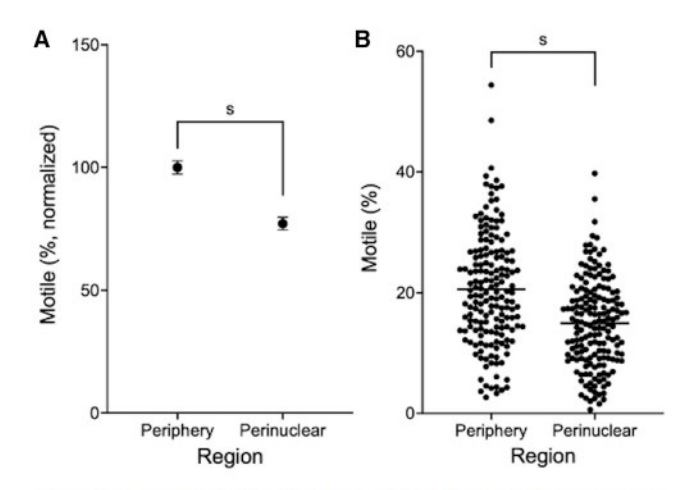


FIGURE 6 Vesicles in the cell periphery are more motile than in the perinuclear region. (A) Average motility of periphery (n=37,106 segments from 9316 trajectories) and perinuclear (n=27,780 segments from 7984 trajectories) regions, normalized to cell periphery. Error bars show 95% CIs. Significance is determined by CIs that do not overlap. (B) Vesicle motility for each region (n=173 cells for both regions). Horizontal lines are means. The significance comparison is taken directly from population-level 95% CIs in (A).

be due to regional differences in the function and organization of actin (111–113) and the ER (114).

#### CONCLUSION

Using single-particle tracking fluorescence microscopy and our previously described Bayesian change-point method (45), we explored how disruption of transport-related cellular structures affects vesicle motility. We found that inhibition of actin and microtubule polymerization resulted in significant decreases in motility (Figs. 1 and 2), as expected. Surprisingly, we found that palmitate-mediated cisternal expansion of the ER resulted in a significant decrease in motility (Fig. 3). We observed no significant change to motility as a result of decreasing ribosome concentration (Fig. 4). In addition, we found that vesicles in the cell periphery were more motile than those in the perinuclear region (Fig. 6), in agreement with our previous results (45).

Overall, our observation that ER disruption results in a large perturbation to vesicle motility suggests that the ER is important in understanding the dynamics of intracellular transport (Fig. 5). Previous work has shown that the ER is important for the positioning of endolysosomal vesicles through a tethering mechanism (50,51). It is possible that the palmitate-mediated disruption of the ER alters this tethering. In addition, palmitate leads to significant cellular stresses, such as mitochondrial dysfunction (96,97) and calcium dysregulation (98,99), which may cause changes in vesicle motility, although MTT and ATP levels were not altered (Figs. S2 and S4). In future work, it will be important to consider the implications for human health and disease. The concentration of fatty acids is elevated in the blood of people with type 2 dia-

betes mellitus (T2DM) (115–118), and T2DM is associated with ER stress (119,120). Further, primary mouse neuronal models of T2DM have been shown to have decreased axonal transport (121,122), and primary adipocytes from type 2 diabetics showed decreased GLUT4 vesicle trafficking (123). These observations all suggest the possibility that ER disruption may be a factor in the transport-mediated effects of T2DM.

#### SUPPORTING MATERIAL

Supporting material can be found online at https://doi.org/10.1016/j.bpj. 2023.03.001.

#### **AUTHOR CONTRIBUTIONS**

N.T.R. and C.K.P. conceived the experiments; N.T.R. conducted the experiments; K.J.C. and S.A.M. provided the code for analysis; and N.T.R. analyzed the results. N.T.R. and C.K.P. wrote the manuscript. All authors reviewed the manuscript.

#### **ACKNOWLEDGMENTS**

This research was supported by the NSF-Simons Southeast Center for Mathematics and Biology (SCMB) through NSF-DMS1764406 and Simons Foundation-SFARI 594594.

#### **DECLARATION OF INTERESTS**

The authors declare no competing interests.

## REFERENCES

- 1. Alberts, B. 1994. Molecular Biology of the Cell. Garland Pub..
- Mogre, S., A. I. Brown, and E. F. Koslover. 2020. Getting around the cell: physical transport in the intracellular world. *Phys. Biol.* 17:061003.
- Vale, R. D. 2003. The molecular motor toolbox for intracellular transport. Cell. 112:467–480.
- Barlan, K., M. J. Rossow, and V. I. Gelfand. 2013. The journey of the organelle: teamwork and regulation in intracellular transport. Curr. Opin. Cell Biol. 25:483

  –488.
- Palm, W., and C. B. Thompson. 2017. Nutrient acquisition strategies of mammalian cells. *Nature*. 546:234–242.
- Sorkin, A., and M. von Zastrow. 2009. Endocytosis and signalling: intertwining molecular networks. Nat. Rev. Mol. Cell Biol. 10:609–622.
- Misgeld, T., and T. L. Schwarz. 2017. Mitostasis in neurons: maintaining mitochondria in an extended cellular architecture. *Neuron*. 96:651–666.
- Lee, M. C. S., E. A. Miller, ..., R. Schekman. 2004. Bi-directional protein transport between the ER and Golgi. Annu. Rev. Cell Dev. Biol. 20:87–123.
- Schwarz, D. S., and M. D. Blower. 2016. The endoplasmic reticulum: structure, function and response to cellular signaling. *Cell. Mol. Life Sci.* 73:79–94.
- Presley, J. F., N. B. Cole, ..., J. Lippincott-Schwartz. 1997. ER-to-Golgi transport visualized in living cells. *Nature*. 389:81–85.
- Glotzer, M. 2005. The molecular requirements for cytokinesis. Science. 307:1735–1739.

- Karki, S., and E. L. Holzbaur. 1999. Cytoplasmic dynein and dynactin in cell division and intracellular transport. Curr. Opin. Cell Biol. 11:45–53.
- Baluska, F., D. Menzel, and P. W. Barlow. 2006. Cytokinesis in plant and animal cells: endosomes 'shut the door'. Dev. Biol. 294:1–10.
- Grafstein, B., and D. S. Forman. 1980. Intracellular transport in neurons. *Physiol. Rev.* 60:1167–1283.
- Goldstein, A. Y. N., X. Wang, and T. L. Schwarz. 2008. Axonal transport and the delivery of pre-synaptic components. *Curr. Opin. Neuro*biol. 18:495–503.
- Guzik, B. W., and L. S. B. Goldstein. 2004. Microtubule-dependent transport in neurons: steps towards an understanding of regulation, function and dysfunction. *Curr. Opin. Cell Biol.* 16:443–450.
- Hirokawa, N., S. Niwa, and Y. Tanaka. 2010. Molecular motors in neurons: transport mechanisms and roles in brain function, development, and disease. *Neuron*. 68:610–638.
- Zhao, Q., S. M. Gao, and M. C. Wang. 2020. Molecular mechanisms of lysosome and nucleus communication. *Trends Biochem. Sci.* 45:978–991.
- Kast, D. J., and R. Dominguez. 2017. The cytoskeleton-autophagy connection. Curr. Biol. 27:R318–R326.
- Yu, L., Y. Chen, and S. A. Tooze. 2018. Autophagy pathway: cellular and molecular mechanisms. *Autophagy*. 14:207–215.
- Dias, C., and J. Nylandsted. 2021. Plasma membrane integrity in health and disease: significance and therapeutic potential. *Cell Discov.* 7:4.
- Corrotte, M., and T. Castro-Gomes. 2019. Lysosomes and plasma membrane repair. Curr. Top. Membr. 84:1–16.
- Cooper, S. T., and P. L. McNeil. 2015. Membrane repair: mechanisms and pathophysiology. *Physiol. Rev.* 95:1205–1240.
- Aridor, M., and L. A. Hannan. 2000. Traffic jam: a compendium of human diseases that affect intracellular transport processes. *Traffic*. 1:836–851.
- Aridor, M., and L. A. Hannan. 2002. Traffic jams II: an update of diseases of intracellular transport. *Traffic*. 3:781–790.
- Staff, N. P., E. E. Benarroch, and C. J. Klein. 2011. Neuronal intracellular transport and neurodegenerative disease. *Neurology*. 76:1015–1020.
- Stokin, G. B., and L. S. B. Goldstein. 2006. Axonal transport and Alzheimer's disease. *Annu. Rev. Biochem.* 75:607–627.
- Ebneth, A., R. Godemann, ..., E. Mandelkow. 1998. Overexpression of tau protein inhibits kinesin-dependent trafficking of vesicles, mitochondria, and endoplasmic reticulum: implications for Alzheimer's disease. J. Cell Biol. 143:777-794.
- Caviston, J. P., and E. L. F. Holzbaur. 2009. Huntingtin as an essential integrator of intracellular vesicular trafficking. *Trends Cell Biol*. 19:147-155.
- Harjes, P., and E. E. Wanker. 2003. The hunt for huntingtin function: interaction partners tell many different stories. *Trends Biochem. Sci.* 28:425–433.
- Nesterova, G., and W. A. Gahl. 1993. Cystinosis. In GeneReviews((R)). M. P. Adam, D. B. Everman, G. M. Mirzaa, R. A. Pagon, S. E. Wallace, L. J. H. Bean, K. W. Gripp, and A. Amemiya, eds.
- Cherqui, S., and P. J. Courtoy. 2017. The renal Fanconi syndrome in cystinosis: pathogenic insights and therapeutic perspectives. *Nat. Rev. Nephrol.* 13:115–131.
- Vale, R. D. 1987. Intracellular transport using microtubule-based motors. Annu. Rev. Cell Biol. 3:347–378.
- Vale, R. D., and R. A. Milligan. 2000. The way things move: looking under the hood of molecular motor proteins. Science. 288:88–95.
- Goldstein, L. S., and Z. Yang. 2000. Microtubule-based transport systems in neurons: the roles of kinesins and dyneins. *Annu. Rev. Neuro*sci. 23:39–71.

- Caviston, J. P., and E. L. F. Holzbaur. 2006. Microtubule motors at the intersection of trafficking and transport. *Trends Cell Biol*. 16:530–537.
- Bálint, Š., I. Verdeny Vilanova, ..., M. Lakadamyali. 2013. Correlative live-cell and superresolution microscopy reveals cargo transport dynamics at microtubule intersections. *Proc. Natl. Acad. Sci. USA*. 110:3375–3380.
- Burute, M., and L. C. Kapitein. 2019. Cellular logistics: unraveling the interplay between microtubule organization and intracellular transport. Annu. Rev. Cell Dev. Biol. 35:29–54.
- Schafer, D. A. 2002. Coupling actin dynamics and membrane dynamics during endocytosis. Curr. Opin. Cell Biol. 14:76–81.
- Langford, G. M. 2002. Myosin-V, a versatile motor for short-range vesicle transport. *Traffic*. 3:859–865.
- Krendel, M., and M. S. Mooseker. 2005. Myosins: tails (and heads) of functional diversity. *Physiology*. 20:239–251.
- Hartman, M. A., and J. A. Spudich. 2012. The myosin superfamily at a glance. J. Cell Sci. 125:1627–1632.
- de Araujo, M. E. G., G. Liebscher, ..., L. A. Huber. 2020. Lysosomal size matters. *Traffic*. 21:60–75.
- Bandyopadhyay, D., A. Cyphersmith, ..., C. K. Payne. 2014. Lysosome transport as a function of lysosome diameter. *PLoS One*. 9:e86847.
- Rayens, N. T., K. J. Cook, ..., C. K. Payne. 2022. Transport of lysosomes decreases in the perinuclear region: insights from changepoint analysis. *Biophys. J.* 121:1205–1218.
- Zhou, H. X., G. Rivas, and A. P. Minton. 2008. Macromolecular crowding and confinement: biochemical, biophysical, and potential physiological consequences. *Annu. Rev. Biophys.* 37:375–397.
- Mourão, M. A., J. B. Hakim, and S. Schnell. 2014. Connecting the dots: the effects of macromolecular crowding on cell physiology. *Biophys. J.* 107:2761–2766.
- Nettesheim, G., I. Nabti, ..., G. T. Shubeita. 2020. Macromolecular crowding acts as a physical regulator of intracellular transport. *Nat. Phys.* 16:1144–1151.
- Sabharwal, V., and S. P. Koushika. 2019. Crowd control: effects of physical crowding on cargo movement in healthy and diseased neurons. Front. Cell. Neurosci. 13:470.
- Bonifacino, J. S., and J. Neefjes. 2017. Moving and positioning the endolysosomal system. Curr. Opin. Cell Biol. 47:1–8.
- Jongsma, M. L. M., I. Berlin, ..., J. Neefjes. 2016. An ER-associated pathway defines endosomal architecture for controlled cargo transport. Cell. 166:152–166.
- Rowland, A. A., P. J. Chitwood, ..., G. K. Voeltz. 2014. ER contact sites define the position and timing of endosome fission. *Cell*. 159:1027–1041.
- Parutto, P., J. Heck, ..., D. Holcman. 2022. High-throughput superresolution single-particle trajectory analysis reconstructs organelle dynamics and membrane reorganization. *Cell Rep. Methods*. 2:100277.
- van der Kant, R., A. Fish, ..., J. Neefjes. 2013. Late endosomal transport and tethering are coupled processes controlled by RILP and the cholesterol sensor ORPIL. J. Cell Sci. 126:3462–3474.
- Ba, Q., G. Raghavan, ..., G. Yang. 2018. Whole-cell scale dynamic organization of lysosomes revealed by spatial statistical analysis. *Cell Rep.* 23:3591–3606.
- Saxton, M. J., and K. Jacobson. 1997. Single-particle tracking: applications to membrane dynamics. *Annu. Rev. Biophys. Biomol. Struct.* 26:373–399.
- Manzo, C., and M. F. Garcia-Parajo. 2015. A review of progress in single particle tracking: from methods to biophysical insights. *Rep. Prog. Phys.* 78:124601.
- Shen, H., L. J. Tauzin, ..., C. F. Landes. 2017. Single particle tracking: from theory to biophysical applications. *Chem. Rev.* 117:7331–7376.

- Sokolov, I. M. 2012. Models of anomalous diffusion in crowded environments. Soft Matter. 8:9043–9052.
- Qian, H., M. P. Sheetz, and E. L. Elson. 1991. Single particle tracking. Analysis of diffusion and flow in two-dimensional systems. *Biophys. J.* 60:910–921.
- Ruthardt, N., D. C. Lamb, and C. Bräuchle. 2011. Single-particle tracking as a quantitative microscopy-based approach to unravel cell entry mechanisms of viruses and pharmaceutical nanoparticles. *Mol. Ther.* 19:1199–1211.
- Michalet, X. 2010. Mean square displacement analysis of single-particle trajectories with localization error: brownian motion in an isotropic medium. *Phys. Rev. E Stat. Nonlin. Soft Matter Phys.* 82:041914.
- 63. Kepten, E., A. Weron, ..., Y. Garini. 2015. Guidelines for the fitting of anomalous diffusion mean square displacement graphs from single particle tracking experiments. *PLoS One*. 10:e0117722.
- Monnier, N., S. M. Guo, ..., M. Bathe. 2012. Bayesian approach to MSD-based analysis of particle motion in live cells. *Biophys. J.* 103:616–626.
- Karslake, J. D., E. D. Donarski, ..., J. S. Biteen. 2021. SMAUG: analyzing single-molecule tracks with nonparametric Bayesian statistics. *Methods*. 193:16–26.
- Chen, Z., L. Geffroy, and J. S. Biteen. 2021. NOBIAS: analyzing anomalous diffusion in single-molecule tracks with nonparametric Bayesian inference. Front. Bioinform. 1:742073.
- Monnier, N., Z. Barry, ..., M. Bathe. 2015. Inferring transient particle transport dynamics in live cells. *Nat. Methods.* 12:838–840.
- Persson, F., M. Lindén, ..., J. Elf. 2013. Extracting intracellular diffusive states and transition rates from single-molecule tracking data. Nat. Methods. 10:265–269.
- Das, R., C. W. Cairo, and D. Coombs. 2009. A hidden Markov model for single particle tracks quantifies dynamic interactions between LFA-1 and the actin cytoskeleton. *PLoS Comput. Biol.* 5:e1000556.
- Granik, N., L. E. Weiss, ..., Y. Shechtman. 2019. Single-particle diffusion characterization by deep learning. *Biophys. J.* 117:185–192.
- Argun, A., G. Volpe, and S. Bo. 2021. Classification, inference and segmentation of anomalous diffusion with recurrent neural networks. J. Phys. A: Math. Theor. 54:294003.
- Gentili, A., and G. Volpe. 2021. Characterization of anomalous diffusion classical statistics powered by deep learning (CONDOR). J. Phys. A: Math. Theor. 54:314003.
- Tinevez, J. Y., N. Perry, ..., K. W. Eliceiri. 2017. TrackMate: an open and extensible platform for single-particle tracking. *Methods*. 115:80–90.
- Hacker, U., R. Albrecht, and M. Maniak. 1997. Fluid-phase uptake by macropinocytosis in Dictyostelium. J. Cell Sci. 110 (Pt 2):105–112.
- Racoosin, E. L., and J. A. Swanson. 1992. M-CSF-induced macropinocytosis increases solute endocytosis but not receptor-mediated endocytosis in mouse macrophages. J. Cell Sci. 102 (Pt 4):867–880.
- Humphries, W. H., 4th, C. J. Szymanski, and C. K. Payne. 2011. Endo-lysosomal vesicles positive for Rab7 and LAMP1 are terminal vesicles for the transport of dextran. *PLoS One*. 6:e26626.
- Delarue, M., G. P. Brittingham, ..., L. J. Holt. 2018. mTORC1 controls phase separation and the biophysical properties of the cytoplasm by tuning crowding. *Cell.* 174:338–349.e20.
- Karaskov, E., C. Scott, ..., A. Volchuk. 2006. Chronic palmitate but not oleate exposure induces endoplasmic reticulum stress, which may contribute to INS-1 pancreatic beta-cell apoptosis. *Endocri*nology. 147:3398–3407.
- Guo, W., S. Wong, ..., Z. Luo. 2007. Palmitate modulates intracellular signaling, induces endoplasmic reticulum stress, and causes apoptosis in mouse 3T3-L1 and rat primary preadipocytes. Am. J. Physiol. Endocrinol. Metab. 293:E576–E586.
- Park, M., A. Sabetski, ..., G. Sweeney. 2015. Palmitate induces ER stress and autophagy in H9c2 cells: implications for apoptosis and adiponectin resistance. J. Cell. Physiol. 230:630–639.

- Kim, S. K., E. Oh, ..., G. T. Chae. 2015. Palmitate induces cisternal ER expansion via the activation of XBP-1/CCTalpha-mediated phospholipid accumulation in RAW 264.7 cells. *Lipids Health Dis.* 14:73.
- Borradaile, N. M., X. Han, ..., J. E. Schaffer. 2006. Disruption of endoplasmic reticulum structure and integrity in lipotoxic cell death. J. Lipid Res. 47:2726–2737.
- Schliwa, M. 1982. Action of cytochalasin D on cytoskeletal networks. J. Cell Biol. 92:79–91.
- Casella, J. F., M. D. Flanagan, and S. Lin. 1981. Cytochalasin D inhibits actin polymerization and induces depolymerization of actin filaments formed during platelet shape change. *Nature*. 293:302–305.
- Hoebeke, J., G. Van Nijen, and M. De Brabander. 1976. Interaction of oncodazole (R 17934), a new antitumoral drug, with rat brain tubulin. *Biochem. Biophys. Res. Commun.* 69:319–324.
- 86. De Brabander, M., G. Geuens, ..., J. De Mey. 1986. Microtubule dynamics during the cell cycle: the effects of taxol and nocodazole on the microtubule system of Pt K2 cells at different stages of the mitotic cycle. *Int. Rev. Cytol.* 101:215–274.
- Vasquez, R. J., B. Howell, ..., L. Cassimeris. 1997. Nanomolar concentrations of nocodazole alter microtubule dynamic instability in vivo and in vitro. *Mol. Biol. Cell.* 8:973–985.
- Pike Winer, L. S., and M. Wu. 2014. Rapid analysis of glycolytic and oxidative substrate flux of cancer cells in a microplate. *PLoS One*. 9:e109916.
- Hidalgo, M., and E. K. Rowinsky. 2000. The rapamycin-sensitive signal transduction pathway as a target for cancer therapy. *Oncogene*. 19:6680–6686.
- Dumont, F. J., and Q. Su. 1996. Mechanism of action of the immunosuppressant rapamycin. *Life Sci.* 58:373–395.
- Iwenofu, O. H., R. D. Lackman, ..., J. S. J. Brooks. 2008. Phospho-S6 ribosomal protein: a potential new predictive sarcoma marker for targeted mTOR therapy. Mod. Pathol. 21:231–237.
- Tee, A. R., and J. Blenis. 2005. mTOR, translational control and human disease. Semin. Cell Dev. Biol. 16:29–37.
- Suh, J., M. Dawson, and J. Hanes. 2005. Real-time multiple-particle tracking: applications to drug and gene delivery. Adv. Drug Deliv. Rev. 57:63–78.
- Erdman, C., and J. W. Emerson. 2007. Bcp: an R package for performing a bayesian analysis of change point problems. J. Stat. Softw. 23:1–13.
- Minin, A. A. 1997. Dispersal of Golgi apparatus in nocodazoletreated fibroblasts is a kinesin-driven process. J. Cell Sci. 110 (Pt 19):2495–2505.
- Lambertucci, R. H., S. M. Hirabara, ..., T. C. Pithon-Curi. 2008. Palmitate increases superoxide production through mitochondrial electron transport chain and NADPH oxidase activity in skeletal muscle cells. J. Cell. Physiol. 216:796–804.
- Han, J., and R. J. Kaufman. 2016. The role of ER stress in lipid metabolism and lipotoxicity. J. Lipid Res. 57:1329–1338.
- Ly, L. D., S. Xu, ..., K. S. Park. 2017. Oxidative stress and calcium dysregulation by palmitate in type 2 diabetes. *Exp. Mol. Med.* 49:e291.
- Xu, S., S. M. Nam, ..., K. S. Park. 2015. Palmitate induces ER calcium depletion and apoptosis in mouse podocytes subsequent to mitochondrial oxidative stress. *Cell Death Dis*. 6:e1976.
- 100. Li, H., Y. Xiao, ..., Z. G. Zhou. 2018. Adipocyte fatty acid-binding protein promotes palmitate-induced mitochondrial dysfunction and apoptosis in macrophages. Front. Immunol. 9:81.
- 101. Sparagna, G. C., D. L. Hickson-Bick, ..., J. B. McMillin. 2000. A metabolic role for mitochondria in palmitate-induced cardiac myocyte apoptosis. Am. J. Physiol. Heart Circ. Physiol. 279:H2124– H2132.
- 102. Listenberger, L. L., D. S. Ory, and J. E. Schaffer. 2001. Palmitate-induced apoptosis can occur through a ceramide-independent pathway. J. Biol. Chem. 276:14890–14895.

- 103. Baker, N. A., D. Sept, ..., J. A. McCammon. 2001. Electrostatics of nanosystems: application to microtubules and the ribosome. *Proc. Natl. Acad. Sci. USA*. 98:10037–10041.
- 104. Li, J., S. G. Kim, and J. Blenis. 2014. Rapamycin: one drug, many effects. Cell Metab. 19:373–379.
- 105. Kennedy, B. K., and D. W. Lamming. 2016. The mechanistic target of rapamycin: the grand ConducTOR of metabolism and aging. *Cell Metab.* 23:990–1003.
- 106. Barilli, A., R. Visigalli, ..., O. Bussolati. 2008. In human endothelial cells rapamycin causes mTORC2 inhibition and impairs cell viability and function. *Cardiovasc. Res.* 78:563–571.
- Bell, E., X. Cao, J. A. Moibi, ..., B. A. Wolf. 2003. Rapamycin has a deleterious effect on MIN-6 cells and rat and human islets. *Diabetes*. 52:2731–2739.
- Kaksonen, M., C. P. Toret, and D. G. Drubin. 2006. Harnessing actin dynamics for clathrin-mediated endocytosis. *Nat. Rev. Mol. Cell Biol.* 7:404

  –414.
- Lambrechts, A., K. Gevaert, ..., M. Van Troys. 2008. Listeria comet tails: the actin-based motility machinery at work. *Trends Cell Biol*. 18:220–227.
- 110. Orth, J. D., E. W. Krueger, ..., M. A. McNiven. 2002. The large GTPase dynamin regulates actin comet formation and movement in living cells. *Proc. Natl. Acad. Sci. USA*. 99:167–172.
- Davidson, P. M., and B. Cadot. 2021. Actin on and around the nucleus. Trends Cell Biol. 31:211–223.
- 112. Luxton, G. W. G., E. R. Gomes, ..., G. G. Gundersen. 2010. Linear arrays of nuclear envelope proteins harness retrograde actin flow for nuclear movement. *Science*. 329:956–959.
- 113. Shao, X., Q. Li, ..., G. V. Shivashankar. 2015. Mechanical stimulation induces formin-dependent assembly of a perinuclear actin rim. Proc. Natl. Acad. Sci. USA. 112:E2595–E2601.

- 114. Puhka, M., H. Vihinen, ..., E. Jokitalo. 2007. Endoplasmic reticulum remains continuous and undergoes sheet-to-tubule transformation during cell division in mammalian cells. J. Cell Biol. 179:895–909.
- 115. Boden, G. 1999. Free fatty acids, insulin resistance, and type 2 diabetes mellitus. Proc. Assoc. Am. Physicians. 111:241–248.
- 116. Bergman, R. N., and M. Ader. 2000. Free fatty acids and pathogenesis of type 2 diabetes mellitus. *Trends Endocrinol. Metab.* 11:351–356.
- 117. Palomer, X., J. Pizarro-Delgado, ..., M. Vázquez-Carrera. 2018. Palmitic and oleic acid: the Yin and Yang of fatty acids in type 2 diabetes mellitus. *Trends Endocrinol. Metab.* 29:178–190.
- 118. Paolisso, G., P. A. Tataranni, ..., E. Ravussin. 1995. A high concentration of fasting plasma non-esterified fatty acids is a risk factor for the development of NIDDM. *Diabetologia*. 38:1213–1217.
- 119. Back, S. H., and R. J. Kaufman. 2012. Endoplasmic reticulum stress and type 2 diabetes. Annu. Rev. Biochem. 81:767–793.
- Eizirik, D. L., A. K. Cardozo, and M. Cnop. 2008. The role for endoplasmic reticulum stress in diabetes mellitus. *Endocr. Rev.* 29:42–61.
- Rumora, A. E., S. I. Lentz, ..., E. L. Feldman. 2018. Dyslipidemia impairs mitochondrial trafficking and function in sensory neurons. FA-SEB J. 32:195–207.
- Rumora, A. E., G. LoGrasso, ..., E. L. Feldman. 2019. Chain length of saturated fatty acids regulates mitochondrial trafficking and function in sensory neurons. J. Lipid Res. 60:58–70.
- 123. Maianu, L., S. R. Keller, and W. T. Garvey. 2001. Adipocytes exhibit abnormal subcellular distribution and translocation of vesicles containing glucose transporter 4 and insulin-regulated aminopeptidase in type 2 diabetes mellitus: implications regarding defects in vesicle trafficking. J. Clin. Endocrinol. Metab. 86:5450–5456.